AIAA JOURNAL
Vol. 47, No. 12, December 2009

Validation of an Inverse Semi-Analytical Technique to Educe Liner Impedance

T. Elnady*
Ain Shams University, 11517 Cairo, Egypt
H. Bodén†
KTH Royal Institute of Technology, 100 44 Stockholm, Sweden
and
B. Elhadidi‡
Cairo University, 12613 Giza, Egypt

DOI: 10.2514/1.41647

In this paper, the acoustic impedance of a liner is educed by a novel semi-analytical inverse technique. The liner sample is placed flush with the solid walls in a rectangular duct with grazing flow. The technique uses complex acoustic pressure measured at four positions at the wall of the duct, upstream and downstream of the lined section, and educes the impedance with a mode-matching method. Previous studies neglected grazing flow nonuniformity and the pressure discontinuity that appears at the liner-wall boundary caused by the discontinuity of the acoustic particle velocity into the wall. In the present paper, the mode-matching formulation is rederived in terms of pressure instead of velocity potential which is found to be more numerically stable. Moreover, the proposed methodology is validated with benchmark data from an experiment performed by NASA. First, the ability of the code to reproduce the pressure field for a given impedance is tested. Second, the ability to educe the correct impedance for a given pressure distribution is tested. The results of the mode-matching code are in very good agreement with the experimental data. The effect of shear flow is investigated and it can be concluded that the assumption of uniform flow is appropriate for the chosen liner, duct size, and frequency range of interest.

Nomenclature

A	=	admittance of the liner, 1/rayl
a	=	half the width of the duct, m
$a_+^{(q)}$, $a_-^{(q)}$	=	amplitudes of the incident and reflected qth mode in the inlet hard duct, Pa
$b_+^{(q)}$, $b_-^{(q)}$	=	amplitudes of the incident and reflected qth mode in the lined duct, Pa
$c_+^{(q)}$, $c_-^{(q)}$	=	amplitudes of the incident and reflected qth mode in the outlet hard duct, Pa
j	=	complex unity
k	=	normalized wave number $= (\omega/c) \cdot a$
$k_m^{(q)}$, $k_n^{(q)}$	=	normalized transversal wave number in the x and y directions, respectively
$k_z^{(q)}$	=	normalized axial wave number of the qth mode
L	=	normalized length of the lined duct
M	=	flow Mach number
p	=	temporal Fourier transform of the pressure, Pa
q	=	mode number
u, w	=	unsteady velocity field in the x and y directions, respectively, m/s
x, y, z	=	normalized Cartesian coordinates $x := x/a$; z coordinate in the direction of the duct axis
$\psi^{(q)}$	=	two-dimensional mode shape of the qth mode after separating the z dependence

Presented as Paper 2639 at the 12th AIAA/CEAS Aeroacoustics Conference, Boston, IL, 8–10 May 2006; received 16 October 2008; revision received 8 July 2009; accepted for publication 19 August 2009.

*Assistant Professor, Ain Shams University Sound and Vibration Laboratory, Faculty of Engineering, Design and Production Engineering Department, 1 Elsarayat Street, Abbaseya. Member AIAA.

†Associate Professor, Aeronautical and Vehicle Engineering Department, Linné Flow Centre, Marcus Wallenberg Laboratory for Sound and Vibration Research, Teknikringen 8. Member AIAA.

‡Assistant Professor, Aerospace Department, Faculty of Engineering. Member AIAA.

I. Introduction

AIRCRAFT engines are major contributors to the overall aircraft noise. In modern high-bypass turbofan engines the nacelle, bypass, and exhaust ducts are acoustically treated with liners to reduce fan-generated noise. To fully benefit from the liner duct treatment in future aircraft engines, it will be necessary to optimize liner treatment design. Such optimization will depend on the ability to accurately predict liner impedance properties for a given liner geometry and design by use of suitable analytical, semi-empirical, and/or numerical models. All models need to be validated by comparing with experimental results, even though semi-empirical models use experimental results as a part of the model development process. A continuing concern in treatment technology is the accurate determination of the normal incidence impedance of an acoustic material subject to grazing flow which is known to add many complications to the measurements.

The normal incidence acoustic impedance of passive linear materials can be experimentally determined in several ways. The first known method is the standing wave tube method which has been a commonly used procedure for impedance measurements for over 80 years [1]. The development of fast Fourier algorithms and its implementation in laboratory analyzers provided new possibilities. The standing wave method evolved to an easier and more accurate method using fixed microphone positions, the two-microphone technique. Seybert and Ross [2] were able to separate the incident and reflected wave spectra from measurements of auto- and cross-spectral densities between the microphones. This method has been used extensively and has become an International Organization for Standardization method [3]. A modified version of this method is used in this paper to decompose the acoustic fields in the hard ducts before and after the lined section, to determine the reflection coefficient perpendicular to the duct axis.

Another very widely used method is the in situ technique. Dean [4] introduced this method in 1974 and, since then, it has been

extensively used to measure the impedance of locally reacting acoustic liners with and without flow. Several drawbacks and problems have been reported with the use of this method. There are usually strong near-field effects which influence the reading of the surface microphone. These effects are even stronger with grazing flow. Moreover, the in situ method becomes more complicated when there is, for example, porous material inside the liner so that the sound propagation inside the cavity is more difficult to predict.

Another trend in acoustic liner impedance measurement technology is the use of indirect approaches, which depend only on the measurement of the acoustic pressure at selected locations outside the liner. These indirect methods have an extra advantage of not destroying the sample by drilling holes for the transducers which requires precision instrumentation of the liner sample. Inverse techniques based on propagation models for the lined duct are therefore becoming popular because of their convenience and advantages.

The classical approach, the so-called infinite-waveguide method, involves measuring the sound attenuation properties of an assumed single, unidirectional propagating mode, in a waveguide lined with the acoustic material over a sufficient length to be effectively infinite. These data are then used with the solution to the wave equation in an infinite waveguide to establish the impedance of the material at the boundary. The evolution of waveguide models for this purpose began over 20 years ago with a uniform mean flow model [5]. Infinite-waveguide models are applicable, in a very straightforward manner, to situations for which a single mode propagates within the waveguide containing the unknown material. However, many conventional liner concepts generate more complex acoustic fields. Thus, measured data must now be interpreted as the superposition of many propagating modes.

Watson et al. [6] developed this approach further and presented a finite-element-based numerical method for educing the impedance of an acoustic material placed at the wall of a two-dimensional duct that conveys a multimodal sound field. Their proposed method depends on the measurement of acoustic pressure at selected locations at the upper wall of a rectangular duct to determine the normal incidence impedance of the material placed at the lower wall. These measurements are then used as input to a finite element propagation model to extract the impedance of the material. They first tested the method with input data computed from modal theory and contaminated by random error. Then they validated the impedance extraction method using measured data and a finite length liner [7]. Later, Watson et al. [8] used the Davidon-Fletcher-Powell optimization algorithm to educe the impedance that minimizes the difference between the measured and the numerically computed upper wall pressure. After developing and validating the method for the no-flow case, they could reproduce the measured normal incidence impedance in a uniform flow [9]. They later showed that the liner resistance educed in the presence of shear flow can differ from that educed when only uniform flow is modeled [10]. The effect of shear flow on the reactance of the liner was not significant. They developed their code further to be able to handle segmented liners in the circumferential and axial directions (checkerboard liners) [11]. Further development of their code has included optimization of the position of the microphones for acoustic pressure measurements [12] and an investigation of the problems occurring near antiresonances or the cut on of higher-order modes [13].

Leroux et al. [14] proposed a method based on the measurement of the scattering matrix of the lined section using the two-source method. The transmission and reflection coefficients before and after the lined section can be calculated from the transfer matrix. They proposed a new theoretical model called "Scattering Matrix by Multimodal Method" to compute the scattering matrix of a lined duct with flow. The basis of this method is to project the propagation equations on a complete set of basis functions. They used uniform mean flow reasoning that shear flow does not affect the transmission coefficients. In their first attempt, they used a minimization criteria based on any of the measured scattering matrix coefficients. Different coefficients resulted in different values for the liner admittance. Allam and Åbom [15] published a different technique based on the transfer matrix to determine the impedance of a perforated wall connecting a duct with flow and a surrounding cavity with extended reaction.

Elnady and Bodén [16] developed a semi-analytical indirect method to determine the acoustic impedance of a liner sample, placed inside a rectangular duct with grazing flow, from measurement of complex acoustic pressure at several positions inside the duct. The amplitude of the plane wave incident toward the lined section and the reflection coefficient at the exit plane are required as input to the model for sound propagation through the lined section. The coupling at the liner inlet and outlet was handled using mode matching. The impedance value which gives the best match between the calculated sound field and the measured one was found using an optimization technique. In this technique, the flow was assumed uniform, whereas any real duct flow will be nonuniform. Furthermore, it is assumed that there is both continuity of pressure and axial particle velocity at the boundary for mode matching between the adjacent ducts. These two assumptions together may result in some errors close to the hard–soft and soft–hard boundaries. These erroneous assumptions result in a discontinuity of the pressure profile at these points matching points. Elnady and Bodén [16] assumed that the pressure field away from this discontinuity represents the actual pressure field, and that the mode-matching code can be used to determine the correct liner impedance. The results in this paper will be compared to the experimental work by Jones et al. [17]. In their experiment, they published data for the evaluation of aeroacoustic propagation codes with grazing flow for different liners, Mach numbers, and frequency.

In this paper, we will first perform a straightforward validation of the code. Using the strength of the incident pressure wave, the exit impedance, and the liner impedance as input data, the pressure profile in the lined section is calculated. The calculated pressure profile at the wall opposite to the liner is then compared to the measured pressure magnitude and phase. Then, an inverse validation is shown. The input data in this case are the strength of the incident pressure wave, the exit impedance, and the pressure profile. The model predicts the impedance using an optimization technique and is then compared with the benchmark data [17]. In this paper, we will show that only the data from four microphones are needed to properly educe the liner impedance. Two of these are placed upstream of the liner and the remaining two downstream. To enhance the numerical stability in the mode-matching technique, a novel formulation for the mode matching is developed based on the pressure as the independent variable instead of the velocity potential. It was found that the new formulation is more stable and can determine the correct impedance more accurately.

In a previous investigation, Watson et al. [18] suggested that including shear flow effects in their finite element code improved the results. Pridmore-Brown [19] also noted that the effects of the mean flow shear are important and should be taken into account. It was shown that the downstream propagating modes refract into the narrow boundary layer at the wall. However, this effect is frequency dependent and is only relevant at high frequencies. Brooks and McAlpine [20] recently published a paper on the prediction of sound transmission in a lined annular duct with sheared mean flow where mode matching was used to determine the sound power transmission loss. It is therefore of interest to include the effects of shear flow in the analytical mode-matching code to investigate how this will influence the results. This will also be of importance for the problem of the discontinuity in the pressure field at the hard–soft boundary. For uniform mean flow in a duct, the unsteady duct modes can be evaluated iteratively using the dispersion relation [21] for the appropriate wall conditions. However, for nonuniform flow, the unsteady modes must be obtained numerically by solving the linearized Euler equations as an eigenvalue problem. Such an eigenvalue problem will yield three discrete sets of solutions: hydrodynamic modes, surface modes, and acoustic modes. The hydrodynamic modes typically represent the rotational (vortical) disturbances and incoming gusts, and are referred to as nearly convected modes, because they are almost pressureless [22]. There can be a maximum of four surface modes [23]. Such modes are characterized by high pressure at the liner surface that decays rapidly in the duct. The acoustic modes

propagate downstream and upstream and are typically characterized by large pressure content. In this paper, we examined the sensitivity of the acoustic modes (axial wave numbers and pressure mode shapes) to the shear flow profile at the frequencies of interest to investigate the validity of the mean flow approximations.

II. Theory

The wave propagation across the lined section inside the duct is described in Fig. 1. The sound source produces an incident plane wave p_{1i}, which travels toward the lined section and is scattered at $z = 0$ into a reflected p_{1r} and transmitted p_{2i} wave. The waves propagating in the lined duct are further scattered at $z = L$ into reflected p_{2r} and transmitted waves p_{3i}. The transmitted wave is further reflected giving p_{3r} at the outlet side of the test rig. The numbering of the fields is as follows: 1 for the inlet hard duct, 2 for the lined duct, and 3 for the outlet hard duct. The letter i refers to the incident wave and the letter r refers to the reflected one. A stationary problem is considered in which all the fields and their derivatives are time harmonic with $e^{j\omega t}$. When the direction of the mean flow is in the axial direction, the wave equation for uniform flow reduces to

$$\nabla^2 p - \left(jk + M\frac{\partial}{\partial z}\right)^2 p = 0 \tag{1}$$

The wave numbers are scaled as $k := ka$ and, consequently, the distances are scaled as $x := x/a$, where a is the duct hydraulic radius. Every solution of the eigenvalue equation corresponds to a propagating mode, each satisfying the same wave equation and boundary conditions. The acoustic field is a summation of all incident and reflected modes.

A. Duct Modes with Uniform Flow

In the inlet and outlet ducts, the cross section is rectangular and all walls are hard. The modes can be easily calculated assuming that the normal particle velocity vanishes at all walls. Because the boundary conditions are symmetric, symmetric and antisymmetric modes can exist in each direction. For symmetric modes, $\partial p(x,0)/\partial y = 0$ and the mode shape is $2\cos(k_n y)$. For antisymmetric modes, $p(x,0) = 0$ and the mode shape is $2j\sin(k_n y)$. Consequently, the normalized wave numbers in the x and y directions are

$$k_m = m\pi/2 \quad \text{and} \quad k_n = n\pi/2 \quad \text{where } m, n = 0, 1, 2, \ldots \tag{2}$$

The dimensions of the hard ducts are chosen together with the frequency range so that only plane waves are allowed to propagate. This condition is necessary for the two-microphone method [24] to be applied. This means that only plane waves can be incident in the inlet duct $a_+^{(1)}$ and reflected in the outlet duct $c_-^{(1)}$. All other higher-order modes in the hard ducts, which are generated at the interfaces with the lined section ($a_-^{(q)}$ and $c_+^{(q)}$), decay exponentially with the axial distance. Nevertheless, they exist in the vicinity of the interfaces and have to be taken into account. The acoustic fields in the inlet and outlet ducts are thus given by

$$p_1(x,y,z) = a_+^{(1)} \cdot \psi_{2i}^{(1)} \cdot e^{-jk_{z2i}^{(1)} \cdot z} + \sum_{q=1}^{Q} a_-^{(q)} \cdot \psi_1^{(q)} \cdot e^{jk_{z1r}^{(q)} \cdot z} \tag{3}$$

and

$$p_3(x,y,z) = \sum_{q=1}^{Q} c_+^{(q)} \cdot \psi_3^{(q)} e^{-jk_{z3i}^{(1)} \cdot (z-L)} + c_-^{(1)} \cdot \psi_3^{(1)} \cdot e^{jk_{z3r}^{(q)} \cdot (z-L)} \tag{4}$$

where $\psi_1^{(q)}$ and $\psi_3^{(q)}$ are identical and given by

$$\psi_1^{(q)} = \psi_3^{(q)} = \begin{Bmatrix} 2\cos(k_{m1}^{(q)} x) \\ 2j\sin(k_{m1}^{(q)} x) \end{Bmatrix} \begin{Bmatrix} 2\cos(k_n^{(q)} y) \\ 2j\sin(k_n^{(q)} y) \end{Bmatrix} \tag{5}$$

In the intermediate lined duct, the liner is placed at $x = -1$ (Fig. 2). In the y direction, the situation is similar to the hard duct, and the wave numbers in this direction k_n can be found from Eq. (2). In the x direction, the boundary conditions are not symmetric. At $x = 1$, the wall is hard and, at $x = -1$, the duct is lined with a locally reacting liner. In the presence of inviscid mean flow, the velocity perturbations at the wall differ from those near the wall. Therefore, Myers [25] corrected for this effect and showed that the fluid particle displacement near the wall is equal to the wall particle displacement. This is an acceptable assumption when plug flow is assumed. The boundary conditions can be written as

$$\partial p/\partial x|_{x=1} = 0 \tag{6}$$

and

$$\partial p/\partial x|_{x=-1} = jkA\left(1 - j\frac{M}{k}\frac{\partial}{\partial z}\right)^2 p|_{x=-1} \tag{7}$$

Substituting the modal expansion into the two boundary conditions, one gets the eigenvalue equation

$$k_{m2}\tan(2k_{m2}) - j\frac{A}{k}(k_{m2}^2 + k_{z2}^2)^2 = 0 \tag{8}$$

which is combined with the dispersion relation

$$k_{z2} = \frac{k}{1-M^2}\left[-M \pm \sqrt{1-(1-M^2)\frac{k_{m2}^2}{k^2}}\right] \tag{9}$$

to find the wave numbers in the x direction k_{m2}. Each mode in the lined duct is finally represented by

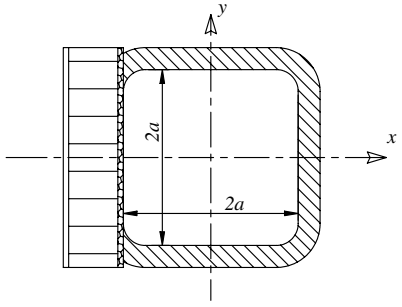

Fig. 2 Cross section in the lined duct.

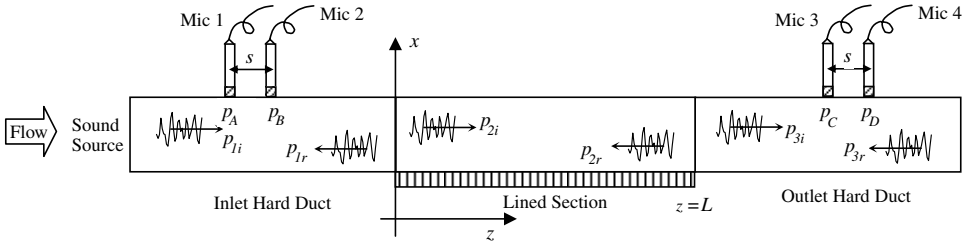

Fig. 1 Incident, reflected and transmitted waves in the calculation domain.

$$p_2^{(q)} = b^{(q)}[e^{jk_{m2}^{(q)}x} + e^{-jk_{m2}^{(q)}(x-2)}]\left\{\begin{matrix}2\cos(k_n^{(q)}y)\\ 2j\sin(k_n^{(q)}y)\end{matrix}\right\}e^{-jk_{z2}^{(q)}z} \quad (10)$$

where k_{m2} has two values, one for each direction, k_{m2i} and k_{m2r}. Every solution of the eigenvalue equation corresponds to a propagating mode. The acoustic field is the summation of all incident and reflected modes:

$$p_2 = \sum_{q=1}^{Q} b_+^{(q)} \cdot \psi_{2i}^{(q)} \cdot e^{-jk_{z2i}^{(q)}\cdot z} + \sum_{q=1}^{Q} b_-^{(q)} \cdot \psi_{2r}^{(q)} \cdot e^{jk_{z2r}^{(q)}\cdot(z-L)} \quad (11)$$

where ψ_{2i} and ψ_{2r} are the mode shapes of the incident and reflected waves, respectively.

B. Mode Matching

Because the incident mode p_+ is plane ($m = 0, n = 0$), and there is no change in the impedance at the boundary in the y direction along the duct axis, the k_n wave numbers remain equal to zero. The problem is then reduced to two dimensions. Mode matching is a well-known technique which is used to determine how energy is transferred and scattered between modes at an interface where there is a discontinuity in either duct dimensions or boundary conditions. The formulation presented in [26] is valid for any cross section with flow, as long as the fields in the three ducts are predetermined and provided that the liner in the intermediate duct is of the locally reacting type. The boundary conditions at the interface between two adjacent ducts implies the continuity of acoustic pressure and axial velocity at $z = 0$ and $z = L$

$$p_1(x, y, 0) = p_2(x, y, 0) \quad (12)$$

and

$$p_2(x, y, L) = p_3(x, y, L) \quad (13)$$

$$\sum_{q=1}^{Q} \frac{\partial p_1^{(q)}/\partial z}{(k \mp Mk_{z1}^{(q)})}\bigg|_{z=0} = \sum_{q=1}^{Q} \frac{\partial p_2^{(q)}/\partial z}{(k \mp Mk_{z2}^{(q)})}\bigg|_{z=0} \quad (14)$$

and

$$\sum_{q=1}^{Q} \frac{\partial p_2^{(q)}/\partial z}{(k \mp Mk_{z2}^{(q)})}\bigg|_{z=L} = \sum_{q=1}^{Q} \frac{\partial p_3^{(q)}/\partial z}{(k \mp Mk_{z3}^{(q)})}\bigg|_{z=L} \quad (15)$$

The negative sign is for the waves traveling in the positive z direction and the positive sign for the waves traveling in the negative z direction. According to the theory of relative convergence, the number of considered modes in both ducts must be equal as long as their areas are equal. The acoustic fields are substituted in the boundary conditions (12–15), multiplied by $\psi_1^{(u)}$, where $u = 1, 2, \ldots, Q$, and then integrated over the cross section. After careful manipulation, the axial boundary conditions yield the following set of independent equations

$$a_+^{(1)}\Lambda_{11}^{1u} + \sum_{q=1}^{Q} a_-^{(q)}\Lambda_{11}^{qu} = \sum_{q=1}^{Q} b_+^{(q)}\Lambda_{2i1}^{qu} + \sum_{q=1}^{Q} b_-^{(q)}\Lambda_{2r1}^{qu}e^{-jk_{z2r}^{(q)}\cdot L} \quad (16)$$

$$\sum_{q=1}^{Q} c_+^{(q)}\Lambda_{11}^{qu}[1 + R_e^{(q)}] = \sum_{q=1}^{Q} b_+^{(q)}\Lambda_{2i1}^{qu}e^{-jk_{z2i}^{(q)}\cdot L} + \sum_{q=1}^{Q} b_-^{(q)}\Lambda_{2r1}^{qu} \quad (17)$$

$$\frac{a_+^{(1)}\Lambda_{11}^{1u}k_{z1i}^{(1)}}{k - Mk_{z1i}^{(1)}} - \sum_{q=1}^{Q} \frac{a_-^{(q)}\Lambda_{11}^{qu}k_{z1r}^{(q)}}{k + Mk_{z1r}^{(q)}} = \sum_{q=1}^{Q} \frac{b_+^{(q)}\Lambda_{2i1}^{qu}k_{z2i}^{(q)}}{k - Mk_{z2i}^{(q)}} - \sum_{q=1}^{Q} \frac{b_-^{(q)}\Lambda_{2r1}^{qu}k_{z2r}^{(q)}e^{-jk_{z2r}^{(q)}\cdot L}}{k + Mk_{z2r}^{(q)}} \quad (18)$$

$$\sum_{q=1}^{Q} c_+^{(q)}\Lambda_{11}^{qu}\left(\frac{k_{z3i}^{(q)}}{k - Mk_{z3i}^{(q)}} - \frac{R_e^{(q)}k_{z3r}^{(q)}}{k + Mk_{z3r}^{(q)}}\right) = \sum_{q=1}^{Q} \frac{b_+^{(q)}\Lambda_{2i1}^{qu}k_{z2i}^{(q)}e^{-jk_{z2i}^{(q)}\cdot L}}{k - Mk_{z2i}^{(q)}} - \sum_{q=1}^{Q} \frac{b_-^{(q)}\Lambda_{2r1}^{qu}k_{z2r}^{(q)}}{k + Mk_{z2r}^{(q)}} \quad (19)$$

where $R_e^{(q)}$ is the exit reflection coefficient and is defined as

$$R_e^{(q)} = c_-^{(q)}/c_+^{(q)} \quad (20)$$

It is equal to zero for all modes except the plane mode. Λ is defined as

$$\Lambda_{pv}^{qu} = \int_{-1}^{1}\int_{-1}^{1} \psi_p^{(q)}\psi_v^{(u)}\mathrm{d}x\mathrm{d}y \quad (21)$$

Equations (16–21) are rearranged and written in matrix form as follows

$$\begin{bmatrix} \Lambda_{11}^{qu} & 0 & -\Lambda_{2i1}^{qu} & -\Lambda_{2r1}^{qu}e^{-jk_{z2r}^{(q)}\cdot L} \\ 0 & \Lambda_{31}^{qu}[1 + R_e^{(q)}] & -\Lambda_{2i1}^{qu}e^{-jk_{z2i}^{(q)}\cdot L} & -\Lambda_{2r1}^{qu} \\ -\frac{\Lambda_{11}^{qu}k_{z1r}^{(q)}}{k+Mk_{z1r}^{(q)}} & 0 & -\frac{\Lambda_{2i1}^{qu}k_{z2i}^{(q)}}{k-Mk_{z2i}^{(q)}} & \frac{\Lambda_{2r1}^{qu}k_{z2r}^{(q)}e^{-jk_{z2r}^{(q)}\cdot L}}{k+Mk_{z2r}^{(q)}} \\ 0 & \Lambda_{31}^{qu}\left(\frac{k_{z3i}^{(q)}}{k-Mk_{z3i}^{(q)}} - \frac{R_e^{(q)}k_{z3r}^{(q)}}{k+Mk_{z3r}^{(q)}}\right) & -\frac{\Lambda_{2i1}^{qu}k_{z2i}^{(q)}e^{-jk_{z2i}^{(q)}\cdot L}}{k-Mk_{z2i}^{(q)}} & \frac{\Lambda_{2r1}^{qu}k_{z2r}^{(q)}}{k+Mk_{z2r}^{(q)}} \end{bmatrix} \times \begin{bmatrix} a_-^{(q)} \\ c_+^{(q)} \\ b_+^{(q)} \\ b_-^{(q)} \end{bmatrix} = \begin{bmatrix} -a_+^{(1)}\Lambda_{11}^{1u} \\ 0 \\ -\frac{a_+^{(1)}\Lambda_{11}^{1u}k_{z1i}^{(1)}}{k-Mk_{z1i}^{(1)}} \\ 0 \end{bmatrix} \quad (22)$$

All unknown modal amplitudes are calculated by solving the preceding system of linear equations in $4Q$ unknowns ($a_-^{(q)}$, $c_+^{(q)}$, $b_+^{(q)}$, $b_-^{(q)}$). This requires the knowledge of the complex values of $a_+^{(1)}$ and $R_e^{(1)}$. To achieve the full advantage and speed of the mode-matching method, all integrals are evaluated analytically. One advantage of choosing the eigenfunctions in the hard duct as the basis function is that they are orthogonal: a property which reduces the number of nonzero coefficients. All Λs in Eq. (22) can be evaluated from the following relations:

$$\Lambda_{11}^{qu} = \delta_{qu}\left\{\begin{matrix}64 & u = 0\\ 32 & u = \text{even}\\ -32 & u = \text{odd}\end{matrix}\right\} \quad (23)$$

and

$$\Lambda_{21}^{qu} = \left\{\begin{matrix} 64 & k_{m1}^{(u)} = k_{m2}^{(q)}, u = 0 \\ 32 & k_{m1}^{(u)} = k_{m2}^{(q)}, u = \text{even} \\ -32 & k_{m1}^{(u)} = k_{m2}^{(q)}, u = \text{odd} \\ 0 & k_{m1}^{(u)} \neq 0, k_{m2}^{(q)} = 0 \\ \frac{16}{jk_{m2}^{(q)}}[e^{3jk_{m2}^{(q)}} - e^{-jk_{m2}^{(q)}}] & k_{m1}^{(u)} = 0, k_{m2}^{(q)} \neq 0 \\ \frac{16jk_{m2}^{(q)}}{k_{m1}^{(u)} - k_{m2}^{(q)}}[e^{3jk_{m2}^{(q)}} - e^{-jk_{m2}^{(q)}}]\cos(k_{m1}^{(u)}) & \text{otherwise}, u = \text{even} \\ \frac{-16k_{m2}^{(q)}}{k_{m1}^{(u)} - k_{m2}^{(q)}}[e^{3jk_{m2}^{(q)}} - e^{-jk_{m2}^{(q)}}]\sin(k_{m1}^{(u)}) & \text{otherwise}, u = \text{odd} \end{matrix}\right\} \quad (24)$$

C. Duct Modes with Shear Flow

To examine the effect of flow nonuniformity, the linearized Euler equations will be solved as an eigenvalue problem. The flow is

assumed two dimensional (which is a valid assumption for low frequencies at which no higher-order modes propagate) and isentropic. The linearized Euler equations for time harmonic waves are expressed by

$$\left(jk + M\frac{\partial}{\partial z}\right)\rho_0 u = -\frac{\partial p}{\partial x}$$
$$\left(jk + M\frac{\partial}{\partial z}\right)\rho_0 w + u\rho_0\frac{\partial M}{\partial x} = -\frac{\partial p}{\partial z}$$
$$\left(jk + M\frac{\partial}{\partial z}\right)p + \gamma p_0\left(\frac{\partial u}{\partial x} + \frac{\partial w}{\partial z}\right) = 0 \tag{25}$$

Furthermore, the mean pressure gradients $\partial p_0/\partial x$ have been neglected as typically assumed in the boundary-layer assumptions. Typically, the unsteady velocity and pressure waves are expressed in terms of a normal Fourier mode expansion

$$\begin{Bmatrix} u_x \\ u_z \\ p \end{Bmatrix}(x, z; t) = \int_{-\infty}^{\infty}\sum_{n=1}^{\infty}\begin{Bmatrix} u_n(x) \\ w_n(x) \\ p_n(x) \end{Bmatrix} e^{-jk_z z}\mathrm{d}\omega \tag{26}$$

where n is an integer. Substituting the Fourier expansion into Eq. (25), the linearized Euler equations reduce to the eigenvalue problem

$$jk\rho_0 u + \frac{\partial p}{\partial x} = k_z(jM\rho_0 u)$$
$$jk\rho_0 w + u\rho_0\frac{\partial M}{\partial x} = k_z(jM\rho_0 w + jp)$$
$$jkp + \gamma p_0\frac{\partial u}{\partial x} = k_z(jMp + j\gamma p_0 w) \tag{27}$$

Note that, unlike the case of a uniform axial mean flow, this is not a Sturm–Liouville eigenvalue problem. Therefore, there is no proof of completeness or orthogonality of the eigenfunctions. The boundary conditions on the walls at $x = -1, 1$ are given by Eqs. (6) and (7) and can summarized in the following relation:

$$u = \mp j\frac{A}{k}\left(jk + M\frac{\partial}{\partial z}\right)p \tag{28}$$

where A is the normalized admittance (equal to zero for the hard wall). Here, the negative sign is for $x = 1$. Different numerical techniques can be used to solve this eigenvalue problem (27). A wealth of literature on the numerical analysis of this problem together with a detailed comparison of various numerical approaches can be found in [21]. The finite differences method is the easiest and the simplest numerical method, in which the system of differential equations is discretized giving a system of algebraic equations of the form

$$[A_\lambda]\boldsymbol{\upsilon} = k_z[B_\lambda]\boldsymbol{\upsilon} \tag{29}$$

where $[A_\lambda]$ and $[B_\lambda]$ are matrices resulting from the discretization of the differential equations, $\boldsymbol{\upsilon}$ is a vector of eigenfunctions, and k_z is the eigenvalue. For classical finite difference and finite element techniques, the matrices $[A_\lambda]$ and $[B_\lambda]$ are sparse, however, the accuracy of the solution is poor [22]. Spectral methods, which are typically used with linear eigenvalue problems, have been used in a number of investigations giving good performance [27]. In these methods, the eigenfunctions are represented by a series of functions which represent a complete orthogonal set, like Chebyshev polynomials, ending up with a system of algebraic equations of the form of Eq. (29). This method has exponential convergence and can resolve thin layers of steep gradients. The main two disadvantages of this method are that the matrices $[A_\lambda]$ and $[B_\lambda]$ are not sparse, which may lead to difficulties in solving the eigensystem as the number of grid points increases, and the introduction of some spurious modes. For two-dimensional problems, the increase and penalty in time to compute the eigensystem is not severe. The spurious modes, however, must be eliminated. Such modes are characterized with very high oscillations and are produced by aliasing from the spectral techniques. These modes are best eliminated by verification of the eigenvalues using a shooting technique once the solution is obtained and used as an initial guess to the shooting algorithm [28].

III. Description of the Benchmark Data and Validation Scheme

The grazing incidence tube test section, used in [17], has internal dimensions of 0.051×0.051 m. The length of the measurement section is 0.812 between the entrance plane and the exit plane where the first and last microphones are located. The tube contains an axially centered test liner with a length of 0.406 m. The surface of the test liner forms the upper wall of the flow duct. Elsewhere, the test section side walls are rigid, with a source upstream of the liner and a nearly anechoic termination downstream of the liner. A ceramic tubular liner was used. This liner has been shown to be nearly linear with respect to mean flow velocity and sound pressure level (SPL), and provides an impedance spectrum that varies over a range typically observed in aircraft engine nacelle liners. Data were acquired with 31 microphones mounted flush to the wall opposite the liner. Three microphones were located upstream of the liner, three microphones were located downstream, and the other 25 microphones were located in the lined section.

Several test cases were reported in the provided data for different settings. The sound pressure level at the source plane was 120, 130, and 140 dB. The frequency range was 500–3000 Hz with 100 Hz step. Average Mach numbers were 0, 0.079, 0.172, 0.255, 0.335, and 0.4. Detailed mean flow profiles were acquired at three axial locations along the duct. Numerical integration was used to compute an average Mach number for the selected axial plane. Finally, the average Mach numbers for each of the three axial planes were averaged together to attain the final average Mach number. This is the value which was used with the plug flow assumption.

The analytical educing technique described in the previous section needs the amplitude of the incident pressure wave toward the liner at the liner leading edge and exit reflection coefficient at the liner trailing edge. These quantities are measured using the two-microphone technique on both sides of the lined section. They are then moved to the edges of the liner ($z = 0$ and $z = L$). The first two microphones (positions A and B in Fig. 1) on the upstream side are used to calculate the amplitude of the incident pressure wave at microphone B at $z = -0.1778$ m and then moved to the reference plane at $z = 0$ using

$$a_+^{(1)} = \left(\frac{p_B}{1 + R_B}\right)\cdot e^{-jk_+ z_B} \quad \text{where } R_B = \left(\frac{1 - H_{AB}\cdot e^{jk_+ s}}{H_{AB}\cdot e^{-jk_- s} - 1}\right) \tag{30}$$

where z_B is the distance between point B and the leading edge of the liner. The last two microphones (positions C and D) on the downstream side were used to calculate the reflection coefficient at microphone D and then moved to the trailing edge of the lined section at $z = L$ to obtain the exit reflection coefficient

$$R_e^{(1)} = \left(\frac{1 - H_{CD}\cdot e^{jk_+ s}}{H_{CD}\cdot e^{-jk_- s} - 1}\right)\cdot e^{-j(k_+ + k_-)z_D} \tag{31}$$

where z_D is the distance between microphone D and the trailing edge of the liner. This value was compared to the exit impedance at the exit plane provided in [17]. They were slightly different and it was decided to use the calculated values from equation.

As soon as both $a_+^{(1)}$ and $R_e^{(1)}$ are known, the system of Eqs. (22) can be solved and the pressure field in the entire duct can be determined. The liner impedance should be known at this stage to calculate the wave numbers within the lined section and the mode shapes. In this paper, the validation of the mode-matching educing technique is done in three steps:

1) Straightforward validation of the code: Using the strength of the incident pressure wave, the exit impedance, and the liner impedance educed in [17] as input data, the pressure profile in the lined section

was calculated. The calculated pressure profile was compared to the measured pressures in magnitude and phase at the wall opposite to the liner.

2) Inverse validation of the code: The input data in this case were the strength of the incident pressure wave, the exit impedance, and the pressure profile. The calculated impedance was compared with the educed impedance values provided in [17]. An arbitrary value of the liner impedance $(1 + i)$ was usually used as a starting guess and used to calculate the modes in the lined duct. Mode matching is then performed using the measured $a_+^{(1)}$ and R_e to calculate the acoustic pressure at the wall microphones. The calculated values of the pressure are compared to the measured values. A new value for the impedance at the boundary is set and the same procedure is repeated until the measured wall pressures can be reproduced. A code was developed for using a minimization algorithm with the following cost function:

$$\text{cost} = \sum_{n=1}^{N} |p_n^{\text{measured}} - p_n^{\text{calculated}}| \tag{32}$$

Note that this positive-definite objective function may be interpreted as the difference between the measured acoustic wall pressure and that computed by the mode-matching code. The minimization was performed using the Matlab function "fminsearch" which uses the simplex search method [29]. The simplicity of the original analytical educing technique in [1] was based on the use of only two microphones upstream and two microphones downstream the lined section. These four microphones are necessary and sufficient to resolve the plane wave sound field in the inlet and outlet hard ducts. Therefore, only these microphone readings (instead of 31) were fed to the minimization algorithm.

3) The results from the previous two steps showed good agreement between the mode-matching code and the benchmark data provided by NASA. It was interesting to further investigate the validity of the uniform flow assumption and the sensitivity of the results to shear flow effects. Another code was constructed to solve for the modes in a rectangular duct lined from one side in the presence of shear flow. The shear flow profile was given in [17]. The axial wave numbers and mode shapes were compared to the uniform flow case for some frequencies and flow speeds.

IV. Validation of the Uniform Flow Mode-Matching Technique

The results from the straightforward validation of the code are presented in Figs. 3 and 4. The figures compare magnitude and phase of the measured wall pressures measured at 31 microphone locations given in the benchmark data to the calculated pressures using the mode-matching (MM) code. The calculated results used the $a_+^{(1)}$ and $R_e^{(1)}$ determined using microphones upstream and downstream of the lined section. The impedance fed to the mode-matching code is that provided by NASA, which they educed based on the pressure measurements using a finite element code. The MM code was validated at all test conditions given in the data and an example is shown in Figs. 3 and 4. For each test case, the plot shows the results for three different calculations. The difference is the number of

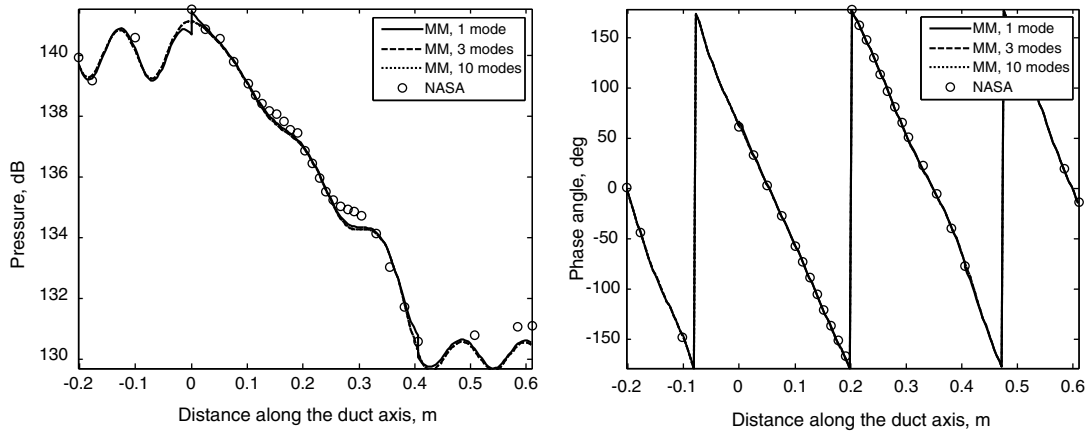

Fig. 3 Comparison of the pressure profile between the mode-matching code and NASA data in [17] at 1500 Hz, $M = 0.079$, incident SPL = 140 dB, and impedance $1.01 + 1.25i$.

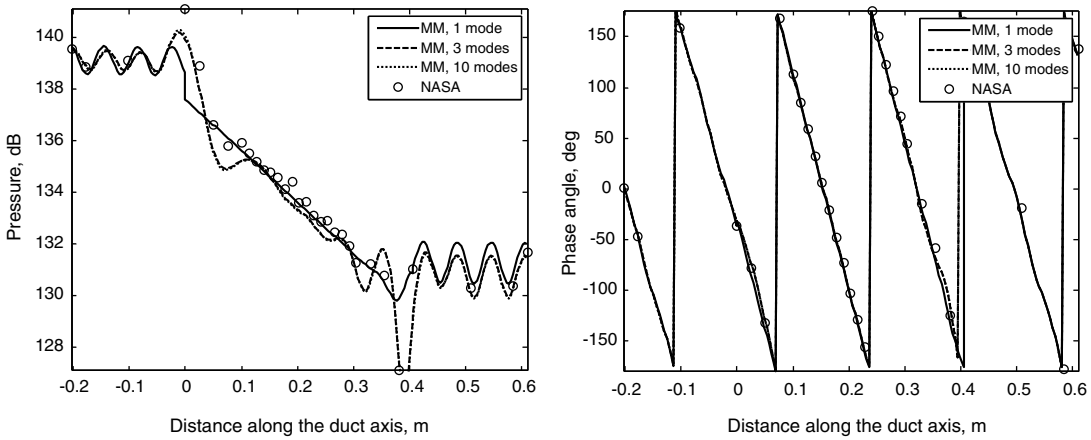

Fig. 4 Comparison of the pressure profile between the mode-matching code and NASA data in [17] at 2500 Hz, $M = 0.335$, incident SPL = 140 dB, and impedance $0.93 - 1.43i$.

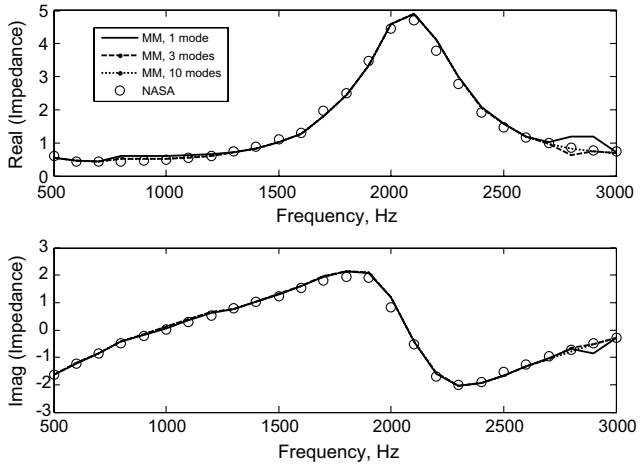

Fig. 5 Comparison of the educed impedance by the mode-matching code and the NASA FEM code using four microphone positions at $M = 0$.

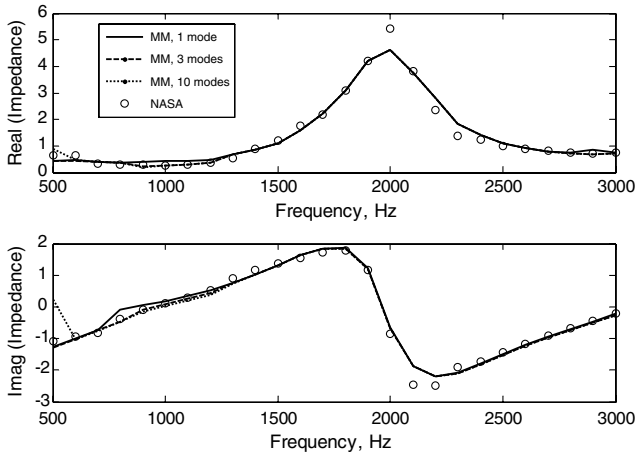

Fig. 6 Comparison of the educed impedance by the mode-matching code and the NASA FEM code using four microphone positions at $M = 0.255$.

modes considered in the field expansion inside the ducts. One, 3, and 10 modes were used. There is hardly any difference between the results using 3 or 10 modes. They are both very similar to the results obtained using only one mode except at the liner edges where there is a discontinuity in the pressure field. Nevertheless, the fields away from the edges are almost identical for the three calculations and in good agreement with the measurement data.

The next step was to perform an inverse validation of the mode-matching code. This means that the code determines the impedance that best reproduces the measured pressure field, as described in Sec. II. It is obvious that increasing the number of microphone positions used in the minimization algorithm should improve the accuracy of predicting the correct impedance.

In the beginning, data from all the 31 microphones provided by NASA in the benchmark data was used. Then, only data from four microphones, the first and last on each side was used. The results were not very different. Figures 5 and 6 show the comparison between the real and imaginary parts of the impedance determined by the mode-matching code and educed by the NASA finite element method (FEM) code. The plots show the result of the mode matching when using 1, 3, or 10 modes in the field expansion. The impedance determined by the mode-matching code agrees well with the impedance given in the benchmark data. There is insignificant difference between the mode-matching results using different number of modes. This indicates that the propagation in the lined section is mainly governed by the attenuation of the fundamental mode.

V. Shear Flow Investigation

In this paper, mode matching has been used to predict the local impedance characteristics of new test liners. Such matching has been based on the assumption of uniform flow and that the effects of nonuniformity are small and negligible. In this section, we wish to examine if such effects are indeed small and can be neglected for the benchmark tests performed, and whether or not there are limitations to such assumptions. A sample of the actual flow profile during one of the measurements in [17] is shown in Fig. 7.

The numerical solution contains hydrodynamic, surface, and acoustic modes. Both hydrodynamic and surface modes must be filtered. As previously mentioned, the hydrodynamic modes are nearly pressureless. Hence, it is possible to filter such modes by examining the normalized pressure eigenvectors and by elimination of the pressureless modes. Furthermore, most of the axial wave numbers of the nearly convected hydrodynamic modes can be found within the range $\omega/U_{\max} \leq k \leq \omega/U_{\min}$. Such a condition is obtained by setting the convected eigenvalue to zero, which is the condition of pure convection. Surface waves are called that way because their pressure field is only significant close to the wall, with very steep exponential decay away from the wall. They are essentially 2-D waves and independent of the duct geometry, and are a consequence of the grazing flow in lined ducts [23]. These modes attenuate rapidly along the duct (high real and imaginary parts associated with the eigenvalue) and are associated with the fluid-structure interaction and surface vibration. Such characteristics make them easily detected. Figure 8 presents the eigenspectrum for one of the test cases. The spectrum clearly contains all three types of modes: acoustic, hydrodynamic, and surface modes.

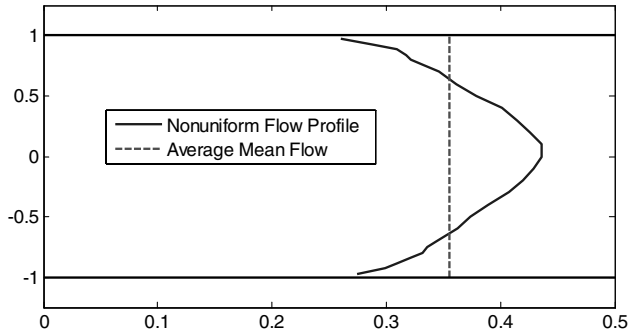

Fig. 7 Shear flow profile of the test case investigated in this paper at the centerline of the duct; mean flow Mach number is 0.335.

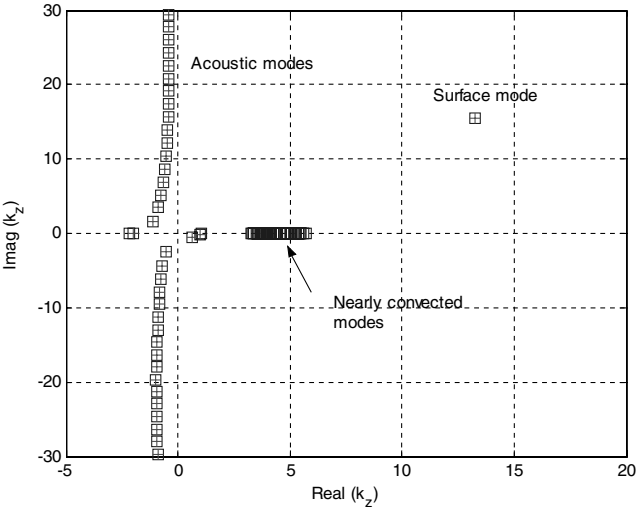

Fig. 8 Eigenspectrum for test case with nonuniform mean flow shown in Fig. 7, $M = 0.335$, $k = 1.4137$, and liner impedance $= 0.73 - 0.24i$.

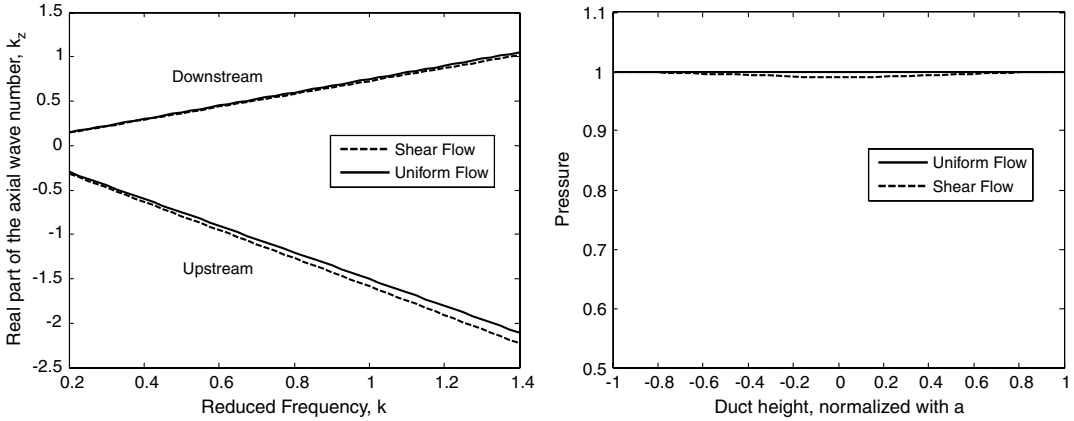

a) Real part of the axial wave number **b) Mode shape at k = 0.8**

Fig. 9 Comparison of the wave numbers and mode shapes of the plane wavelike mode in a hard duct when plug flow is assumed and the shear flow in Fig. 7 is used.

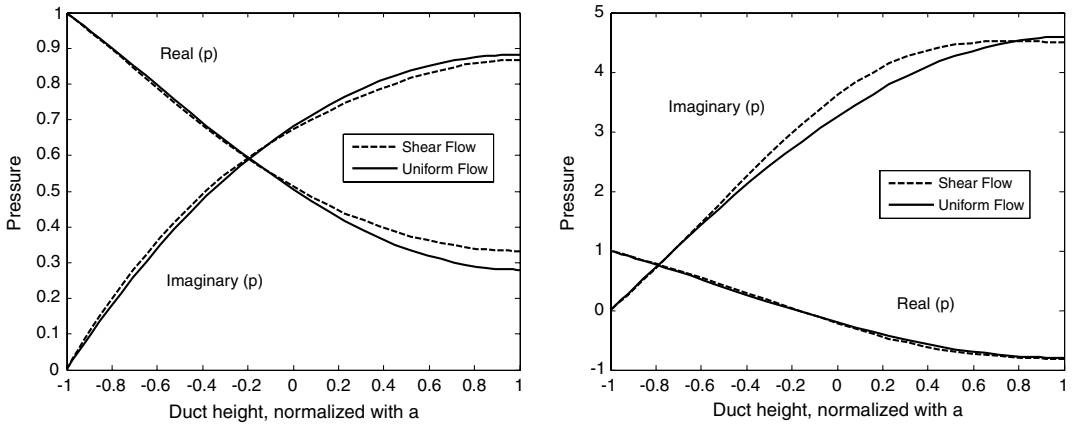

a) First mode **b) Second mode**

Fig. 10 Comparison of the real and imaginary pressure mode shapes when plug flow is assumed and when the shear flow in Fig. 7 is used, $M = 0.335$, $k = 1.4137$, and liner impedance $= 0.73 - 0.24i$.

Figure 9 examines the sensitivity of the eigenvalues and pressure modes to the nonuniform mean flow for the case of hard walled duct. This is important because the acoustic waves propagate in the hard ducts up and downstream the lined section, where the microphone measurements take place. It is clearly seen that, for the range of reduced frequencies considered, the differences in the axial wave number is small and that the pressure modes are nearly plane waves.

Figure 10 compares the pressure modes shape with a line impedance $= 0.73 - 0.24i$, at the highest test frequency of 3000. Again, we see that the differences between the uniform flow approximation and the measured velocity profile are very small. Table 1 compares the axial wave numbers of the first and second modes for plug flow and sheared flow. As evident from the results, the changes in the values are small (less than 5%), especially for the first mode which dominates the propagation inside the duct. This means that these differences would probably have a small effect on the educed impedance.

Table 1 Comparison between the calculated eigenvalues using plug flow and sheared flow

		Uniform plug flow	Sheared flow
First mode	Downstream	$0.9891 - 0.2289i$	$0.9656 - 0.2162i$
	Upstream	$-1.8848 + 0.0704i$	$-2.0065 + 0.0711i$
Second mode	Downstream	$0.7298 - 0.5858i$	$0.6421 - 0.5965i$
	Upstream	$-0.9921 + 1.6497i$	$-1.1373 + 1.6494i$

VI. Conclusions

A semi-analytical technique to measure liner impedance in grazing flow has been presented and validated. This technique uses the measurement of complex acoustic pressure at four positions inside the duct, upstream and downstream the lined section, and calculates the result using the mode-matching method. Benchmark data published by NASA were used for validation. It was shown that the pressure field described by the simple mode-matching technique away from the liner edges is representative of the pressure, and that the code would be capable to educe the correct liner impedance. The results of the mode-matching educed impedance were in good agreement with the experimental data. The effect of shear flow was investigated and it was found that the effect is small for the chosen duct size and frequency range of interest. The numerical solution for the nonuniform mean flow eigenvalue problem indicates that the approximation of plug flow is a reasonable approximation and can be used to educe the liner properties with sufficient accuracy. Such approximations may not be valid for higher frequencies when multiple modes cut on.

Acknowledgments

Part of this work is funded by the Swedish Research Council (Vetenskapsrådet) and the Swedish International Development Cooperation Agency within the Swedish Research Links Program. The other part is funded by the European Commission within the

Tempus Program. The authors would like to thank Michael Jones for providing the benchmark data in electronic format.

References

[1] Acoustics: Determination of Sound Absorption Coefficient and Impedance in Impedance Tubes, Part I: Method Using Standing Wave Ratio, International Organization for Standardization ISO 10534-1, 1996.

[2] Seybert, A. F., and Ross, D. F., "Experimental Determination of Acoustic Properties Using a Two-Microphone Random Excitation Technique," *Journal of the Acoustical Society of America*, Vol. 61, No. 5, 1977, pp. 1362–1370. doi:10.1121/1.381403

[3] Acoustics: Determination of Sound Absorption Coefficient and Impedance in Impedance Tubes, Part 2: Transfer-Function Method, International Organization for Standardization ISO 10534-2, 1998.

[4] Dean, P., "An In-Situ Method of Wall Acoustic Impedance Measurement in Flow Ducts," *Journal of Sound and Vibration*, Vol. 34, No. 1, 1974, pp. 97–130. doi:10.1016/S0022-460X(74)80357-3

[5] Armstrong, D. L., Beckemeyer, R. J., and Olsen, F. R., "Impedance Measurements of Acoustic Duct Liners with Grazing Flow," *Journal of the Acoustical Society of America*, Vol. 55, No. S1, April 1974, p. S59. doi:10.1121/1.1919823

[6] Watson, W. R., Jones, M. G., Tanner, S. E., and Parrot, T. L., "A Finite Element Propagation Model for Extracting Normal Incidence Impedance in Non-Progressive Acoustic Wave Fields," NASA TM-110160, 1995.

[7] Watson, W. R., Jones, M. G., Tanner, S. E., and Parrot, T. L., "Validation of a Numerical Method for Extracting Liner Impedance," *AIAA Journal*, Vol. 34, No. 3, 1996, pp. 548–554. doi:10.2514/3.13102

[8] Watson, W. R., Tanner, S. E., and Parrot, T. L., "Optimization Method for Educing Variable-Impedance Liner Properties," *AIAA Journal*, Vol. 36, No. 1, 1998, pp. 18–23. doi:10.2514/2.369

[9] Watson, W. R., Tanner, S. E., and Parrot, T. L., "Validation of an Impedance Eduction Method in Flow," AIAA Paper 98-2279, 1988.

[10] Watson, W. R., Tracy, M. B., Jones, M. G., and Parrott, T. L., "Impedance Eduction in the Presence of Shear Flow," *7th AIAA/CEAS Aeroacoustics Conference*, AIAA Paper 2001-2263, 28–30 May 2001.

[11] Watson, W. R., Robinson, J., Jones, M. G., and Parrott, T. L., "Design and Attenuation Properties of Periodic Checkerboard Liners," *9th AIAA/CEAS Aeroacoustics Conference*, AIAA Paper 2003-3309, May 2003.

[12] Jones, M. G., Watson, W. R., and Nark, D. M., "Optimization of Acoustic Pressure Measurements for Impedance Eduction," AIAA Paper 2007-3531, May 2007.

[13] Watson, W. R., Jones, M. G., and Parrot, T. L., "Investigation of an Anomaly Observed in Impedance Eduction Techniques," AIAA Paper 2008-3013, May 2008.

[14] Leroux, M., Job, S., Aurégan, Y., and Pagneux, V., "Acoustical Propagation in Lined Duct with Flow: Numerical Simulations and Measurements," *10th International Congress on Sound and Vibration*, P393, July 2003, pp. 3255–3262.

[15] Allam, S., and Åbom, M., "Experimental Characterization of Acoustic Liners with Extended Reaction," AIAA Paper 2008-3074, May 2008.

[16] Elnady, T., and Bodén, H., "An Inverse Analytical Method for Extracting Liner Impedance from Pressure Measurements," AIAA Paper 2004-2836, May 2004.

[17] Jones, M., Watson, W., and Parrott, T., "Benchmark Data for Evaluation of Aeroacoustic Propagation Codes with Grazing Flow," AIAA Paper 2005-2853, May 2005.

[18] Watson, W. R., Tracy, M. B., Jones, M. G., and Parrott, T. L., "Impedance Eduction in the Presence of Shear Flow," AIAA Paper 2001-2263, May 2001.

[19] Pridmore-Brown, D. C., "Sound Propagation in a Fluid Flowing Through an Attenuating Duct," *Journal of Fluid Mechanics*, Vol. 4, No. 4, 1958, pp. 393–406. doi:10.1017/S0022112058000537

[20] Brooks, C. J., and McAlpine, A., "Sound Transmission in Ducts with Sheared Mean Flow," AIAA Paper 2007-3545, May 2007.

[21] Eversman, W., "Theoretical Models for Duct Acoustic Propagation and Radiation," *Aeroacoustics of Flight Vehicles, Theory and Practice*, Acoustical Society of America, New York, 1995.

[22] Ali, A. A., "Aeroacoustics and Stability of Swirling Flows," Ph.D. Thesis, University of Notre Dame, South Bend, IN, 2001.

[23] Rienstra, S. W., "A Classification of Duct Modes Based on Surface Waves," AIAA Paper 2001-2180, May 2001.

[24] Chung, J. Y., and Blaser, D. A., "Transfer Function Method of Measuring In-Duct Acoustic Properties, I: Theory," *Journal of the Acoustical Society of America*, Vol. 68, No. 3, 1980, pp. 907–913. doi:10.1121/1.384778

[25] Myers, M., "On the Acoustic Boundary Condition in the Presence of Flow," *Journal of Sound and Vibration*, Vol. 71, No. 3, 1980, pp. 429–434. doi:10.1016/0022-460X(80)90424-1

[26] Elnady, T., and Bodén, H., "Mode Scattering by Hard Strips in Lined Ducts," *10th International Congress on Sound and Vibration*, P027, July 2003, pp. 621–628.

[27] Golubev, V. V., and Atassi, H. M., "Acoustic Vorticity Waves in Swirling Flows," *Journal of Sound and Vibration*, Vol. 209, No. 2, 1998, pp. 203–222. doi:10.1006/jsvi.1997.1049

[28] Atassi, O. V., and Ali, A. A., "Inflow/Outflow Conditions for Time-Harmonic Internal Flows," *Journal of Computational Acoustics*, Vol. 10, No. 2, 2002, pp. 155–182.

[29] Lagarias, J. C., Reeds, J. A., Wright, M. H., and Wright, P. E., "Convergence Properties of the Nelder-Mead Simplex Method in Low Dimensions," *SIAM Journal on Optimization*, Vol. 9, No. 1, 1998, pp. 112–147. doi:10.1137/S1052623496303470

E. Gutmark
Associate Editor